Impact of the electronic structure on the solubility and diffusion of 3*d* transition elements in silicon

D. Gilles, W. Schröter, and W. Bergholz*
IV. Physikalisches Institut, Universität Göttingen, Bunsenstrasse 11-15, D-3400 Göttingen, Federal Republic of Germany
(Received 10 May 1989)

The dependence of the solubilities and diffusion coefficients of Mn, Fe, and Co on doping with B, P, and As in Si have been studied by the tracer method. An enhancement of the solubility by up to 4 orders of magnitude has been observed for P concentrations greater than 5×10^{18} cm^{-3} and temperatures between 700 °C and 850 °C. The enhancement is due to immobile substitutional 3*d* impurity atoms forming multiple-acceptor centers and pairs with P at those temperatures. By contrast, in intrinsic and highly-B-doped Si, impurities on interstitial sites dominate the solubility, with the exception of Mn for $T<850$ °C. The interstitials act as donor centers resulting in a solubility enhancement for high B dopings ($T<900$ °C, [B] $>5\times10^{18}$ cm^{-3}) due to the singly positive charge state and impurity-boron pairs. No evidence for a dependence of the diffusion coefficient on the charge state has been found. The analysis of the solubility on the Fermi level shows that the donor levels of interstitial Mn, Fe, and Co above 700 °C abruptly shift towards the valence band with temperature. This is the first experimental evidence that a point-defect configuration becomes unstable at high temperatures in analogy to an instability of the Si self-interstitial conjectured by Seeger and Chick [Phys. Status Solidi **29**, 455 (1968)] 20 years ago. It is further proposed that the multiple-acceptor behavior of substitutional Mn, Fe, and Co is due to a strong increase in the vacancy concentration in highly-P-doped Si as compared with intrinsic Si for $T<850$ °C.

I. INTRODUCTION

3*d* transition-element impurities in Si are characterized by deep levels, low solubilities, and high diffusivities[1,2] compared to shallow donor and acceptor impurities. For some of them (Cr,Mn,Fe) an interstitial diffusion mechanism has been verified directly.[1,3] For Co, Ni, and Cu the investigation of the dissolved impurity atoms is severely hampered by a tendency of almost complete precipitation during quenching because of their remarkably high diffusivities coupled with low migration enthalpies.[4–7] The latter property has been considered to be indicative of interstitial diffusion.

Although there is a strong variation of the measured solubilities going along the 3*d* row from Ti to Cu,[1] two groups may be distinguished according to their formation enthalpies ΔH_s with respect to the silicon-richest metal silicide: 3*d*-I (Cr,Mn,Fe,Co; $\Delta H_s\approx2.1$ eV) and 3*d*-II (Ni,Cu; $\Delta H_s\approx1.5$ eV). It has been suggested[1] that 3*d*-I elements dissolve and migrate as neutral interstitial species $M_i^{(0)}$, 3*d*-II elements as positively charged interstitial species $M_i^{(+)}$, and that the difference in the solution enthalpies results from the electronic contribution of $M_i^{(+)}$. However, with the exception of Cu,[4] up to now charge states have always been determined at low temperatures ($T<350$ K) and not at diffusion temperatures ($T>1000$ K). There is no well-established procedure of how to extrapolate them to the diffusion temperature. Moreover, for Co_i and Ni_i, the electronic structure is known from theoretical calculations only.[8,9]

According to Shockley and Moll,[10] possible charge states of an impurity at the diffusion temperature may be determined from the exponential dependence of its equilibrium concentration on the Fermi energy. Whereas the concentration of a neutral species, $M^{(0)}$, is independent of the position of the Fermi energy, the concentrations of the charged impurity species depend on the relative position the Fermi energy, E_F, and the corresponding ionization level, according to

$$\cdots[M^{(-)}]:[M^{(0)}]:[M^{(+)}]:[M^{(2+)}]\cdots = \cdots\exp[(E_F-G^{(-/0)})k_BT]:1:\exp[(G^{(0/+)}-E_F)/k_BT]:\exp[(G^{(0/+)}+G^{(+/2+)}-2E_F)/k_BT]\cdots . \quad (1)$$

$E_c-G^{[n/(n+1)]}$ is the standard chemical potential for ionization from n to $n+1$. E_c denotes the conduction-band edge, T the temperature, and k_B the Boltzmann factor. In regions where the solubility is determined by one charge state, this charge state can be calculated from the slope of a plot of the solubility versus the Fermi energy.

Hall and Racette[4] concluded from the dependence of the solubility and diffusion coefficient of Cu on the B concentration that, in intrinsic and B-doped Si, Cu is positively charged and dissolved predominantly on interstitial sites at or below 700 °C. In highly-P- or As-doped Si the authors interpreted the strong solubility enhancement as

being due to triply negatively charged substitutional Cu, $Cu_s^{(3-)}$.

A difficulty one encounters in applying the simple analysis as used by Hall and Racette comes from neglecting other impurity species. As has been pointed out by Meek and Seidel,[11] pairing of Cu_s with P or As is quite likely, questioning the identification of the charge state of Cu_s.

Our investigation had two aims: (1) to extend the investigation to Mn, Fe, and Co ($3d$-I group), and (2) to take into account the problem of defect reactions in order to extract high-temperature charge states of an impurity species in regions of the Fermi energy where other species of the same impurity might be present in much higher concentrations. One example would be Cu_i in highly-P-doped Si, where the total concentration of Cu is determined by Cu_s, which outnumbers Cu_i. However, under those conditions a separation of mobile species, responsible for the transport, and immobile species which determine the solubility, from diffusion profiles cannot be accomplished for the most general case. We have obtained a separation of impurity species from the analysis of diffusion profiles using the assumptions that local equilibrium between the various impurity species and intrinsic point defects is established [Assumption (A1)] and that the influence of intrinsic point defects, which take part in the transformation, between the different species on the diffusion profiles can be neglected [Assumption (A2)]. Concentration profiles are then expected to be simple, i.e., they can be described by one effective diffusion coefficient D_{eff}:

$$D_{\text{eff}}=\left[\sum_{\alpha,n} D_\alpha^{(n)}[M_\alpha^{(n)}]^{\text{eq}}\right]\Big/ C_{\text{tot}}^{\text{eq}} \ . \tag{2}$$

The summation has to be extended over all impurity species (α) and their charge states (n). $C_{\text{tot}}^{\text{eq}}=\sum_{\alpha,n}[M_\alpha^{(n)}]^{\text{eq}}$ is the solubility with respect to the equilibrium silicide which can be determined from the saturation concentration or surface concentration of diffusion profiles.

$C_{\text{tot}}^{\text{eq}}$ and D_{eff} are the two parameters directly accessible from tracer-diffusion profiles. If the transport of the impurity by diffusion occurs by its interstitial species only, Eq. (2) can be simplified further to

$$C_{\text{tot}}^{\text{eq}}D_{\text{eff}}=\sum_n D_i^{(n)}[M_i^{(n)}]^{\text{eq}} \ . \tag{3}$$

Note that if the interstitial species is neutral, $C_{\text{tot}}^{\text{eq}}D_{\text{eff}}$ does not change with a variation of the Fermi energy.

The consistency of Eqs. (2) and (3) with experiments will be demonstrated in Sec. III. We wish to point out that especially the situation expressed in Assumption (A2) is not always met experimentally. A well-known example is the diffusion of Au in Si.[12–14] For this impurity the concentration of Au_s is assumed to be much larger than that of Au_i, even in intrinsic Si. From the analysis of the Au diffusion profiles, it has been concluded that the Au diffusion is controlled by the transport or the generation of intrinsic point defects which are needed for the transformation $Au_i \leftrightarrow Au_s$.

Our new approach to analyze high-temperature charge states of interstitial impurities is to measure the dependence of $C_{\text{tot}}^{\text{eq}}D_{\text{eff}}$ rather than of $C_{\text{tot}}^{\text{eq}}$ alone, which provides a separation of the electronic properties of mobile and immobile impurity species. It is obvious from Eq. (3) that a measurement of the dependence of $C_{\text{tot}}^{\text{eq}}D_{\text{eff}}$ on the position of the Fermi energy yields information about charge states of an interstitial impurity species independent of other immobile species of the same impurity: The slope $\ln[C_{\text{tot}}^{\text{eq}}D_{\text{eff}}(E_F)]$ is determined by the charge states of the interstitial impurity species. A separation of different immobile species can be accomplished by additional spectroscopic methods, such as, e.g., Mössbauer spectroscopy or deep-level transient spectroscopy (DLTS).

In this work results on the identification of impurity species and their charge states above 700 °C are reported for Mn, Fe, and Co. The Mn and Fe systems have the additional advantage that the electronic levels of Mn_i (Refs. 15–18) and Fe_i (Refs. 16, 19, and 20) at low temperatures are well established, which is not the case for Co_i and Cu_i (for a discussion of the literature data, see Ref. 2): First, it has been one aim of this work to check extrapolation procedures, which yield the energy-level scheme of a point defect at high temperatures from the values at low temperatures. Such extrapolations to high temperatures have been common practice without any real justification.

In this paper striking similarities between the $3d$ transition elements are reported: Mn_i, Fe_i, and Co_i introduce a single donor level into the band gap of Si at 700 °C. These levels shift towards and eventually merge with the valence band between 900 and 1100 °C. This behavior questions any extrapolation from low temperatures and is indicative of a structural change of the point defect. Secondly, from our analysis we propose that, in highly-P-doped Si, Fe_s, Mn_s, and Co_s are dominant because of acceptor states associated with those species. From Mössbauer experiments it is concluded that a major fraction of Co_s forms pairs with P. Thirdly, we have obtained first results on the charge-state dependence of the diffusion coefficient D_i, i.e., on the ratio $D_i^{(0)}/D_i^{(+)}$.

II. EXPERIMENT

Ingots of single-crystalline Si with several doping concentrations [float zone (FZ)—10^{18}–8×10^{19} B-atoms/cm^3, 8×10^{13} P-atoms/cm^3, etch-pit density (EPD) of 0 cm^{-2}, 1×10^{20} P-atoms/cm^3, EDP of $<10^4$ cm^{-2}; Czochralski (CZ)—2×10^{19} As-atoms/cm^3, EPD of 0 cm^{-2}] were cut into specimens of dimensions $11\times11\times(2-4)$ mm^3, the large surfaces oriented along ⟨111⟩ directions. After standard mechanical and chemical polishing, one or both large surfaces were plated with the transition element under study by evaporation of a mixture of the stable and radioactive chloride of the transition element dissolved in HCl. The following radioactive isotopes have been used: ^{59}Fe, ^{54}Mn, ^{57}Co.

For temperatures above 900 °C it was found[1,3] that a thick layer of the metal is required to produce a well-defined boundary condition for diffusion. In that case the surface concentration is equal to the solubility of the transition element with respect to its silicon-richest sili-

cide. The high sensitivity of the tracer method enabled us to extend the measurements of the solubility to a temperature as low as 700 °C. However, from diffusion experiments on Co in intrinsic Si, Utzig and Gilles[7] have concluded that below 900 °C the formation of the equilibrium phase might not be completed for short diffusion times (< 10 min). In most cases we have therefore chosen an annealing time of about 1 d. An exception was highly-B-doped Si because of the large observed diffusion coefficient. However, the solubility changes by doping with shallow impurities have been found to be much higher than the changes caused by the kinetics of the silicide formation.

The diffusion anneals were carried out in an Ar:H_2 (93.5 vol %, 6.5 vol %) ambient in a vertical furnace and terminated by quenching the specimens in diffusion-pump oil. From comparisons with solubility and diffusion data of samples plated by evaporation of a piece of metallic Mn,[3] we have found no influence of the chloride on either the diffusion or the solubility. To avoid any influence of the side faces on the diffusion profile, cylinders with diameters of 9 mm were drilled ultrasonically from the diffusion specimens. The disks were then sectioned into layers about 100 μm thick by grinding on a jig. Concentration profiles were obtained by counting the γ activity of the layers with a Ge γ-spectrometer totally surrounded by a lead shield with a thickness of 100 mm and by determination of the weight loss of the sample after each grinding step on a microbalance. The activity was calibrated by reference sources supplied by New England Nuclear (accuracy ±5%).

For the analysis of experimental solubilities and diffusion coefficients for charge states, the Fermi energy was calculated using the Ehrenberg approximation including the temperature dependence of the band gap,[21] the density of states being taken as $N_c = (5.3\times10^{15}$ atoms/cm$^3)T^{3/2}$,[22] and that of the valence band as $N_v = (2.2\times10^{15}$ atoms/cm$^3)T^{3/2}$.[23] Furthermore, in the charge-neutrality equation the shallow donors and acceptors were assumed to be totally ionized.

For Mössbauer-effect investigations $^{57}CoCl_2$ (without added inactive Co) was dripped onto the samples and the evaporation residue acted as a diffusion source during the annealing treatments. The Mössbauer spectra were recorded on a conventional constant-acceleration drive in transmission geometry with a $K_4Fe(CN)_6\cdot3H_2O$ single-line absorber containing 0.5 mg ^{57}Fe. The full width at half maximum (FWHM) is $\gamma = 0.41$ mm/s [for the B-doped sample a $Na_4Fe(CN)_6\cdot10H_2O$ single-line absorber with $\gamma = 0.355$ mm/s was used instead]. Velocities are quoted relative to the absorber. Before recording the Mössbauer spectra, any residual Co on the surfaces and silicide phases were removed.

III. RESULTS AND DISCUSSION

A. Diffusion profiles, diffusion coefficients, and solubilities

1. Mn in Si

The diffusion of Mn in Si has been measured as a function of the Fermi energy for 1038, 854, and 700 °C. Some representative diffusion profiles are shown in Figs. 1(b), 2(b), and 3(b). The solubilities (●), as determined from the extrapolated surface concentrations or average concentration of saturated specimens as a function of the position of the Fermi energy, are plotted in Figs. 1(a), 2(a), and 3(a). The figures also show the values of $C_{tot}^{eq}D_{eff}$ (○). Note that an increase of C_{tot}^{eq} indicates the introduction of at least one immobile Mn species, if $C_{tot}^{eq}D_{eff}$ remains constant with a variation of the Fermi energy [see, e.g., Fig. 3(a)] and of a charged mobile species, if this product increases.

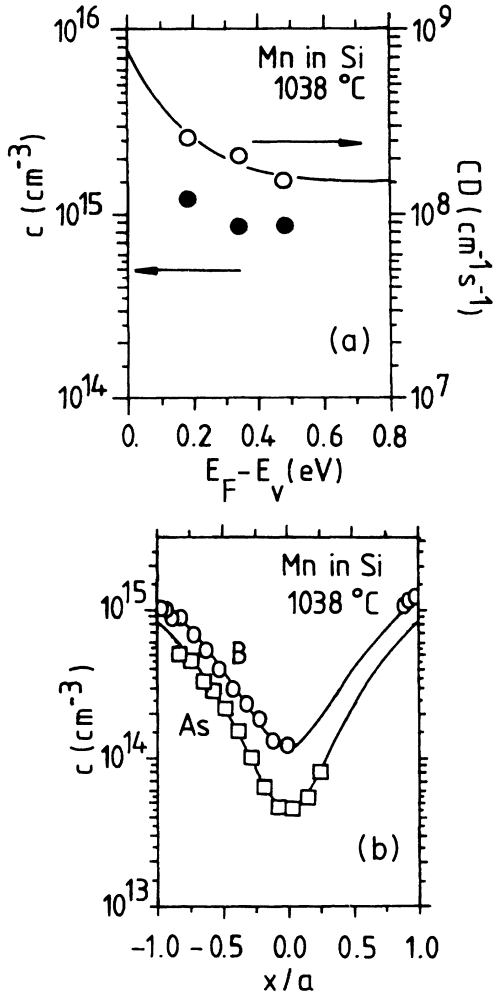

FIG. 1. Solubilities and diffusion profiles of Mn in undoped, B-, and As-doped Si at 1038 °C. (a) The solubilities (●) and products of the solubilities and diffusion coefficients (○) vs the Fermi energy calculated from the diffusion profiles of (b). The solid line represents a numerical fit by Eq. (6) to $C_{tot}^{eq}D_{eff}$. The values obtained in intrinsic Si have been obtained from a sample diffused simultaneously with the B- and P-doped ones and are consistent with the literature. (b) Concentration profiles after in-diffusion from both large surfaces of the specimens, as determined by the radiotracer method. The depth x of each profile is normalized with respect to the thickness $2a$ of the sample. The annealing time was 50 min: ○, 2×10^{19} B-atoms/cm^3, $2a = 0.436$ cm; □, 2×10^{19} As-atoms/cm^3, $2a = 0.451$ cm. The solid lines represent least-squares fits to the solution of the diffusion equation assuming time-independent surface concentrations.

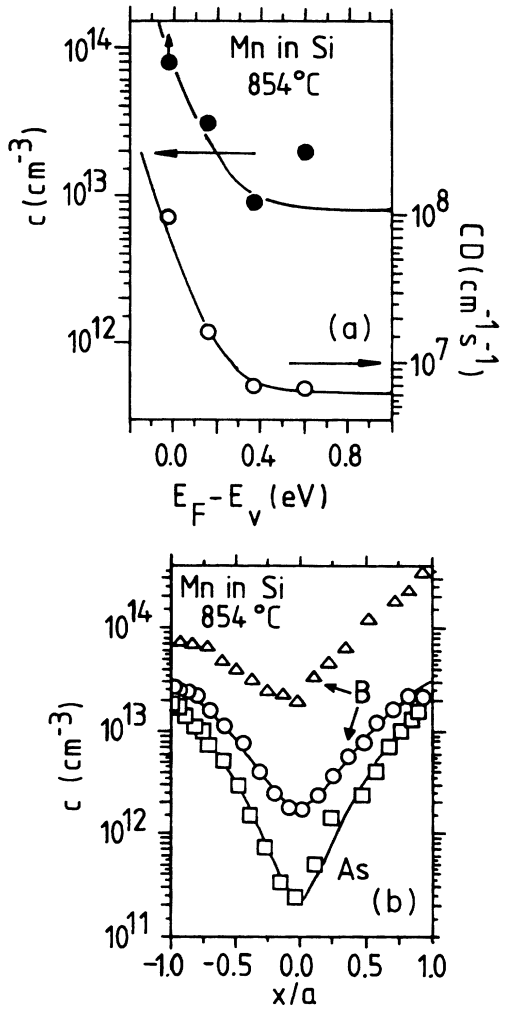

FIG. 2. Solubilities and diffusion profiles of Mn in undoped, B-, and As-doped Si at 854 °C. (a) The solubilities (●) and products of the solubilities and diffusion coefficients (○) vs Fermi energy calculated from the diffusion profiles of (b). The values in intrinsic Si were obtained from a sample simultaneously diffused with the B- and As-doped specimens. The solid lines represent numerical fits by Eq. (6) to $C_{\rm tot}^{\rm eq}D_{\rm eff}$ and of Eq. (5) to $C_{\rm tot}^{\rm eq}$ making use of $[{\rm Mn}_i]^{\rm eq}=[{\rm Mn}_i^{(0)}]$ in n-type Si. From the fits, $\tilde{G}_i^{(0/+)}=G_i^{(0/+)}$ can be concluded, if $[{\rm Mn}_s^{(+)}]\ll[{\rm Mn}_i^{(+)}]$ holds. The solubility in n-type Si is dominated by an immobile species. (b) Concentration profiles after in-diffusion for 102 min from both sides of the specimen, as determined by the tracer method. The depth x of each profile is normalized with respect to the thickness $2a$ of the sample. △, 8×10^{19} B-atoms/cm^3, $2a=0.179$ cm; ○, 2×10^{19} B-atoms/cm^3, $2a=0.369$ cm; □, 2×10^{19} As-atoms/cm^3, $2a=0.374$ cm. For the highest B concentration (△), the difference of the surface concentrations and concentration gradients might be due to a variation of the B concentration within the sample. A separate fit of the two parts of the diffusion profile yields a value of $C_{\rm tot}^{\rm eq}D_{\rm eff}$, which, for the part of the profile with the higher surface concentration, is consistent with the results determined for different Fermi energies. For the left-hand part of the profile the surface concentration and the value of $C_{\rm tot}^{\rm eq}D_{\rm eff}$ is expected for Si doped with 3×10^{19} cm^{-3}. Hence, the value of 8×10^{13} cm^{-3} in that material is certainly an estimation of lower limit for the solubility. The solid lines represent least-squares fits to the solution of the diffusion equation assuming time-independent surface concentrations.

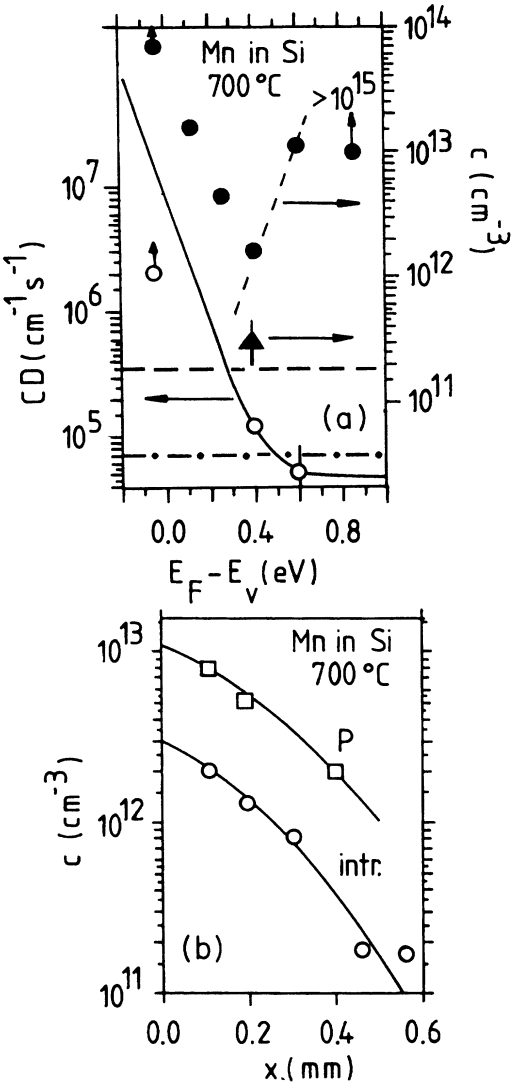

FIG. 3. Solubilities and diffusion profiles of Mn in undoped, B-, and P-doped Si at 700 °C. (a) The solubilities (●) and products of the solubilities and diffusion coefficients (○) vs the Fermi energy. Except in P-doped Si, the solubility values represent saturation concentrations. The solid line is a fit by Eq. (6) to $C_{\rm tot}^{\rm eq}D_{\rm eff}$. In Si+$8\times10^{19}$ B-atoms/cm^3, $C_{\rm tot}^{\rm eq}D_{\rm eff}$ is an estimation of lower limit due to the saturation of the sample. The total concentration might also be larger because of a possible variation of the B content [cf. Fig. 2(b)]. In Si+10^{20} P-atoms/cm^3 the concentration of Mn was below the detection limit at a depth larger than 100 μm after an annealing time of 7 d. The estimation of the diffusion coefficient of below 4×10^{-11} cm^2/s implies the presence of an immobile Mn species, the concentration of which exceeds 10^{15} cm^{-3}. Note that, in Si+5.4×10^{18} P-atoms/cm^3 ($E_F-E_v=0.6$ eV), $C_{\rm tot}^{\rm eq}D_{\rm eff}$ is comparable with the value extrapolated from high temperatures (horizontal dashed-dotted line), although the solubility deviates from the extrapolated value (horizontal dotted line) by up to 2 orders of magnitude. In intrinsic Si, $[{\rm Mn}_i]^{\rm eq}$ as measured by DLTS (▲) is only 0.1–0.2 of the solubility. We presume that in intrinsic and n-type Si the solubility is determined by ${\rm Mn}_s^{(-)}$ (inclined dashed line). (b) Concentration profiles after in-diffusion from one side of the specimen, as determined by the tracer method. The depth x of each profile is normalized with respect to the thickness $2a$ of the sample. □, 5.4×10^{18} P-atoms/cm^3, $t=1$ d; ○, 8×10^{13} P-atoms/cm^3, $t=90$ min.

TABLE I. Impact of the doping with shallow impurities on the diffusion and solubility of Mn in Si. The diffusion coefficient of Si + 10^{20} P-atoms/cm^3 at 700 °C (*) was estimated from the finding that no Mn was detected at a depth larger than 100 μm after annealing for 7 d. The diffusion coefficient and solubility in Si + 8×10^{19} B-atoms/cm^3 at 854 °C (†) were determined from the right-hand part of the diffusion profile shown in Fig. 2(b).

	$T=1038$ °C		$T=854$ °C		$T=700$ °C	
Doping (cm^{-3})	C_{tot}^{eq} (cm^{-3})	D_{eff} (cm^2/s)	C_{tot}^{eq} (cm^{-3})	D_{eff} (cm^2/s)	C_{tot}^{eq} (cm^{-3})	D_{eff} (cm^2/s)
[P] $=1\times10^{20}$						$<4\times10^{-11}$*
[As] $=2\times10^{19}$	8.9×10^{14}	1.68×10^{-6}	2.0×10^{13}	3.75×10^{-7}		
[P] $=5\times10^{18}$					1.1×10^{13}	$(5\pm2)\times10^{-9}$
[P] $=8\times10^{14}$	8.6×10^{14}	2.49×10^{-6}	8.9×10^{12}	8.4×10^{-7}	3.0×10^{12}	$(7\pm1)\times10^{-8}$
[B] $=2\times10^{19}$	8.9×10^{14}	2.08×10^{-6}	3.1×10^{13}	5.86×10^{-7}		
[B] $=8\times10^{19}$			$\approx3\times10^{14}$†	$\approx2.3\times10^{-7}$†		

The following features are immediately obvious from Figs. 1–3 and Table I.

(1) The solubility increases both for heavy *n*- and *p*-type dopings; the effects are more pronounced at lower temperatures.

(2) Heavy *n*-type doping reduces the effective diffusion coefficient.

(3) In B-doped Si there is a dependence of the diffusion coefficient to a much lesser extent than in *n*-type Si, such that doping with B enhances C_{tot}^{eq} as well as $C_{tot}^{eq}D_{eff}$.

Above 900 °C, Mn is dissolved predominantly on interstitial sites.[1,3] As can be seen in Fig. 1(a), the solubility varies only slightly with B- or As-doping at 1038 °C. This means that the dominant species, Mn_i, is neutral at that temperature, i.e., $Mn_i^{(0)}$. At 700 °C, however, the solubility in intrinsic Si exceeds an extrapolation from high temperatures by 1 order of magnitude. At the same time the diffusion coefficient is smaller than the extrapolated value by a factor of 5 (Fig. 4). Therefore at this temperature $Mn_i^{(0)}$ is not the dominant species in intrinsic Si.

2. *Fe in Si*

As for Mn, the solubility of Fe is enhanced for heavy B and P dopings at 700 °C [Fig. 5(a) and Table II]. Going from the highest B doping to the highest P doping, the diffusion coefficient varies by more than 3 orders of magnitude. To relate these measurements to the diffusion coefficient of Fe_i, which up to now has not been measured for 700 °C, we calculated D_i making use of a relation given by Weber:[1]

$$D=(1.3\times10^{-3}\ \text{cm}^2/\text{s})\exp[(-0.68\ \text{eV})/k_BT]\ .$$

This relation has been obtained from a fit to published data in low-doped Si for two temperature regimes, one around room temperature from the pairing and precipitation kinetics of Fe_i, and the other around 1200 °C from tracer measurements. Our value of $D=1.7\times10^{-6}$ cm^2/s at 920 °C obtained from out-diffusion experiments is in good agreement with this relation.[24] The extrapolation to 700 °C ($D_i=4\times10^{-7}$ cm^2/s) is comparable with the value in B-doped Si, but considerably larger than that in P-doped Si. Young[25] has shown that at high temperatures this diffusivity has to be associated with $Fe_i^{(0)}$, since he did not find any influence of doping with shallow donors on the Fe solubility above 900 °C. From an extrapolation of his and Weber's solubility data we obtained $[Fe_i^{(0)}]^{eq}=10^{11}$ cm^{-3} and finally $[Fe_i^{(0)}]^{eq}D_i^{(0)}$ [see Fig. 5(a)].

Note that $[Fe_i^{(0)}]^{eq}D_i^{(0)}$ as calcualted from these extrapolations agrees well with the value of $C_{tot}^{eq}D_{eff}$, as measured for P-doped Si at 700 °C. This means that the dominant Fe species in heavily-P-doped Si immobile.

3. *Co in Si*

Some results of the solubility and the effective coefficient of Co in B- and P-doped Si which have been published previously[26] are presented in Fig. 6 and Table

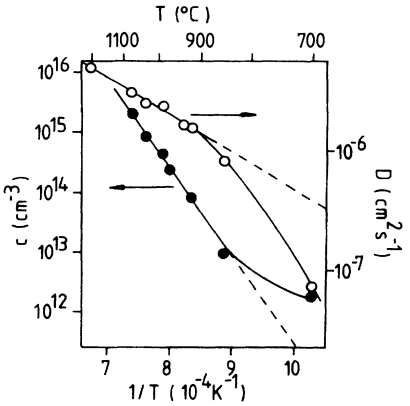

FIG. 4. Temperature dependence of the solubility and diffusion coefficient of Mn in undoped Si. The values above 900 °C were taken from Ref. 3.

TABLE II. Impact of doping with shallow impurities on the diffusion and solubility of Fe in Si at 700 °C. In Si + 10^{20} P-atoms/cm^3 the diffusion coefficient and solubility were obtained from a diffusion profile after annealing for 7 d. The concentration decreased from 8×10^{14} to 2×10^{14} cm^{-3} within 80 μm from the large surfaces of the specimen.

	$T=700$ °C	
Doping (cm^{-3})	C_{tot}^{eq} (cm^{-3})	D_{eff} (cm^2/s)
[P] $=1\times10^{20}$	$(6\pm2)\times10^{14}$	$\approx4\times10^{-11}$
[P] $=8\times10^{14}$	5×10^{11}	
[B] $=8\times10^{19}$	3×10^{13}	2.4×10^{-7}

III. These data will be analyzed further considering a possible charge-state dependence of the diffusivity of interstitial Co. Furthermore, these data are needed to demonstrate common trends in the properties of Mn, Fe, Co, and Cu.

We have omitted the solubility data at 700 °C measured in CZ-Si since we have reasons to suspect that oxygen

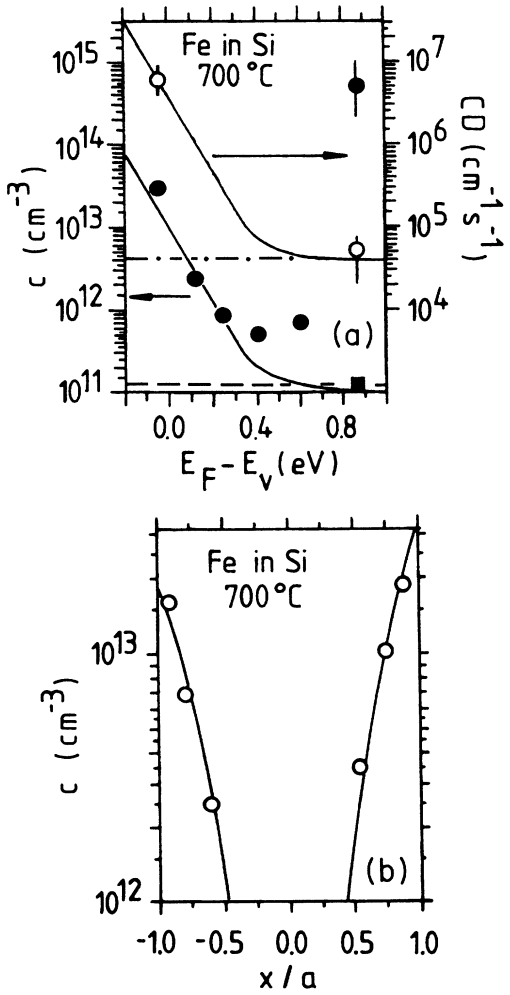

FIG. 5. Solubility and diffusion data of Fe in Si for various dopings with P and B. (a) Solubility (●) and the product of the solubility and diffusion coefficient (○) vs the Fermi energy. In Si + 10^{20} P-atoms/cm^3, an annealing time of 7 d has led to a penetration depth of about 80 μm, corresponding to a diffusion coefficient of about 4×10^{-11} cm^2/s. The surface concentration yields 8×10^{14} cm^{-3}. The value of $C_{tot}^{eq}D_{eff}$ in that material is in agreement with a high-temperature extrapolation of $[Fe_i^{(0)}]^{eq}D_i^{(0)}$ (dashed-dotted horizontal line). Using the value of $D_i^{(0)}$ (Ref. 1), the equilibrium concentration of $Fe_i^{(0)}$ is 10^{11} cm^{-3} (■). The solid lines are fits by Eq. (6) to $C_{tot}^{eq}D_{eff}$ and Eq. (5) to C_{tot}^{eq} with $[Fe_i^{(0)}]^{eq}=10^{11}$ cm^{-3} fixed. The increase of the solubility in n-type Si is due to an immobile Fe species. (b) Concentration profile in Si + 8×10^{19} B-atoms/cm^3 after in-diffusion from both large surfaces of the specimen ($t=28$ min, $2a=0.200$ cm). The depth x of the profile is normalized with respect to the thickness $2a$ of the sample. The solid lines represent a numerical fit to the solution of the diffusion equation assuming different but time-independent surface concentrations. These small differences may be due to a variation of the B-concentration [cf. Fig. 2(b)].

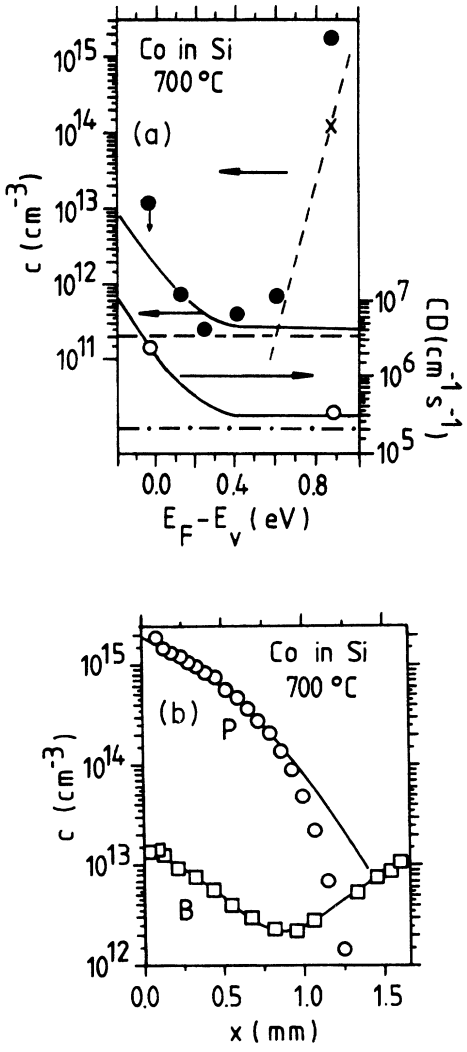

FIG. 6. Solubility and diffusion profiles of Co in Si at 700 °C for various B and P dopings. (a) Solubility (●) and the product of the solubility and diffusion coefficient (○) vs the Fermi energy. For the highest B doping the solubility might be less than the value obtained from the extrapolated surface concentration (factor ≈ 2.5) due to incomplete $CoSi_2$ formation during the short annealing time (see Ref. 7). The value of $C_{tot}^{eq}D_{eff}$ in Si + 10^{20} P-atoms/cm^3 agrees well with the value of $[Co_i^{(0)}]^{eq}D_i^{(0)}$ estimated in undoped Si (dashed-dotted line). The value of C_{tot}^{eq} in intrinsic Si is consistent with the literature (dashed horizontal line). The solid lines are fits by Eq. (6) to $C_{tot}^{eq}D_{eff}$ and Eq. (5) to C_{tot}^{eq}, yielding $\tilde{G}_i^{(0/+)} \approx G_i^{(0/+)}$. The concentration of Co_s in P-doped Si (×) has been calculated from Mössbauer experiments. From the dependence of $[Co_s]$ on the Fermi energy, it is inferred that Co_s is at least twice negatively charged (inclined dotted line). (b) Concentration profiles after in-diffusion from one or both sides of the specimen. ○, 10^{20} P-atoms/cm^3, $t=7$ d, $2a=0.25$ cm. The diffusion coefficient was calculated by a least-squares fit of the complementary error function to the first part of the diffusion profile (see Ref. 26). □, 8×19 B-atoms/cm^3, $t=9$ min. The solid line is a least-squares fit to the solution of the diffusion equation assuming different but time-independent surface concentrations. (The plot in Ref. 26 was in error.)

TABLE III. Impact of doping with shallow impurities on the diffusion and solubility of Co in Si at 700 and 800 °C. In Si + 8×10^{14} P-atoms/cm^3 the value for the diffusion coefficient (*), extrapolated from temperatures between 1100 and 900 °C (Ref. 7), is about the estimation of the lower limit determined from saturation experiments (Ref. 1).

	$T=700$ °C			$T=800$ °C		
Doping (cm^{-3})	C_{tot}^{eq} (cm^{-3})	D_{eff} (cm^2/s)	$C_{tot}^{eq}D_{eff}$ (1/cm s)	C_{tot}^{eq} (cm^{-3})	D_{eff} (cm^2/s)	$C_{tot}^{eq}D_{eff}$ (1/cm s)
[P] = 1×10^{20}	1.8×10^{15}	2×10^{-9}	3.6×10^{6}	4.5×10^{14}	1.2×10^{-7}	5.4×10^{7}
[P] = 8×10^{14}	4×10^{11}	1.1×10^{-5}*	4.4×10^{6}	5.1×10^{12}	1.65×10^{-5}	8.4×10^{7}
[B] = 8×10^{19}	1.5×10^{13}	2.25×10^{-6}	3.4×10^{7}			

precipitation leads to a reduction of the Co solubility in n-type Si as compared to FZ-Si.[27] The solubility for the highest B-doping concentration, as obtained from the surface concentration of a diffusion profile, might have to be corrected for incomplete formation of $CoSi_2$ indicated by the vertical arrow in Fig. 6(a).

It has been shown that (1) there is no influence of B and As on the solubility of Co above 900 °C,[28] and (2) C_{tot}^{eq} in intrinsic Si follows an Arrhenius-type law between 700 and 1100 °C.[1] From these results it can be concluded that $Co_i^{(0)}$ is the dominant species in intrinsic Si above 700 °C.

The results for Co plotted in Fig. 6 show the same trends observed for Fe and Mn: Whereas the solubility enhancement in n-type Si is pronounced and accompanied by a decrease of D_{eff}, the latter is hardly affected by doping with B. The experimental results are consistent with Assumptions (A1) and (A2): The solubility enhancement in P-doped Si at 700 °C by a factor of about 5000 is nearly exactly compensated by a decrease of the diffusion coefficient to give the same value of $C_{tot}^{eq}D_{eff}$ (cf. Table III). At 800 °C that solubility enhancement factor is less than 3 orders of magnitude, but again the same compensation is observed. Thus it can be concluded that the transport is determined by the diffusion of the interstitial species, which, in the case of Co, is neutral in intrinsic and n-type Si at 700 and 800 °C.

B. Results obtained from DLTS and Mössbauer spectroscopy

Comparing the data presented in the preceding section for Mn, Fe, and Co, one notices common trends like the dominance of the neutral interstitial species at temperatures above 900 °C, a strong increase of the solubility with B and P doping at 700 °C, a simultaneous decrease of the diffusivity with P doping, and the agreement of the measured values of $C_{tot}^{eq}D_{eff}$ with the extrapolated values of $D_i^{(0)}[M_i^{(0)}]^{eq}$. Hence we presume that similar atomic and electronic configurations of these elements determine $C_{tot}^{eq}(E_F)$. These similarities also extend in part to Cu. In order to get a more detailed picture of the species involved in the solubility enhancement in B- and P-doped Si, we have used Mössbauer spectroscopy of Co to discriminate the various species by their s-electron densities and field gradients, as well as DLTS to detect Mn-related deep levels in addition to Mn_i. In what follows we shall summarize arguments that in P-doped Si M_s and M_sP and in B-doped Si M_iB pairs significantly influence the solubility of transition-metal impurities below 900 °C.

1. M_s in intrinsic Si and M_s and M_sP in P-doped Si

As for the existence of an immobile substitutional species in P-doped Si, good evidence is furnished by Mössbauer spectroscopy of ^{57}Co: Two new species have been found in Si doped with 10^{20} P-atoms/cm^3 which transform reversibly into each other upon annealing between 600 and 900 °C [Figs. 7(a) and 7(b)]. The single line arising from a species with a cubic environment has been assigned to Co_s due to the low diffusivity of that species ($<2\times10^{-8}$ cm^2/s). The existence of a field gradient and the reversible transformation to Co_s are strong arguments for an identification of the quadrupole doublet as Co_sP. It remains unclear how many P atoms are actually involved in the pair with Co. The concentration ratio of the two species shows an Arrhenius-type behavior [Fig. 7(c)] and yields a binding energy for Co_sP of 1.5 ± 0.1 eV. The total Co concentrations at 700 and 800 °C have been decomposed into $[Co_s]^{eq}$ and $[Co_sP]^{eq}$ and are shown in Fig. 8.

For Fe the variation of the solubility and the diffusion coefficient with the P doping at 700 °C is similar to that found for Co, so that we propose the dominance of Fe_s and Fe_sP in Si + 10^{20} P-atoms/cm^3. We have no direct evidence for the existence of two such species though.

For Mn a P doping of 5×10^{18} atoms/cm^3 significantly enhances the solubility at 700 °C (see Table I), which is not accompanied by a corresponding change of $C_{tot}^{eq}D_{eff}$. This implies an immobile species to be responsible for the solubility enhancement in P-doped Si. There is some independent evidence from DLTS measurements that Mn_s is already the dominant species in intrinsic Si at 700 °C. (i) The electrically active concentration of Mn_i is only a fraction (0.1–0.2) of the solubility as measured by the tracer method. (ii) After in-diffusion of Mn at 942 °C for 36 min, in addition to the two well-established DLTS lines of Mn_i in n-type Si, one line ($L3$) has been found,[3] the concentration of which is proportional to $[Mn_i]$ throughout the diffusion profile (Fig. 9). Lemke has found two defects associated with Mn, whose emission rates are comparable with that measured for line $L3$ (Fig. 10): Mn_iB (Ref. 29) and a line which arises after co-diffusion with Cu and has been attributed to Mn_s.[30] We can exclude Mn_iB since its concentration would be much too high for the specified residual acceptor concentration

(below 4×10^{12} cm^{-3}). Therefore, the DLTS line $L3$ is attributed to Mn_s.

2. M_i and M_iB in B-doped Si

The solubility enhancement of Mn, Fe, and Co [and Cu in B-doped Si (Ref. 4)] could result from $M_i^{(+)}$, $M_s^{(+)}$, and also from their pairs with B, especially M_iB.

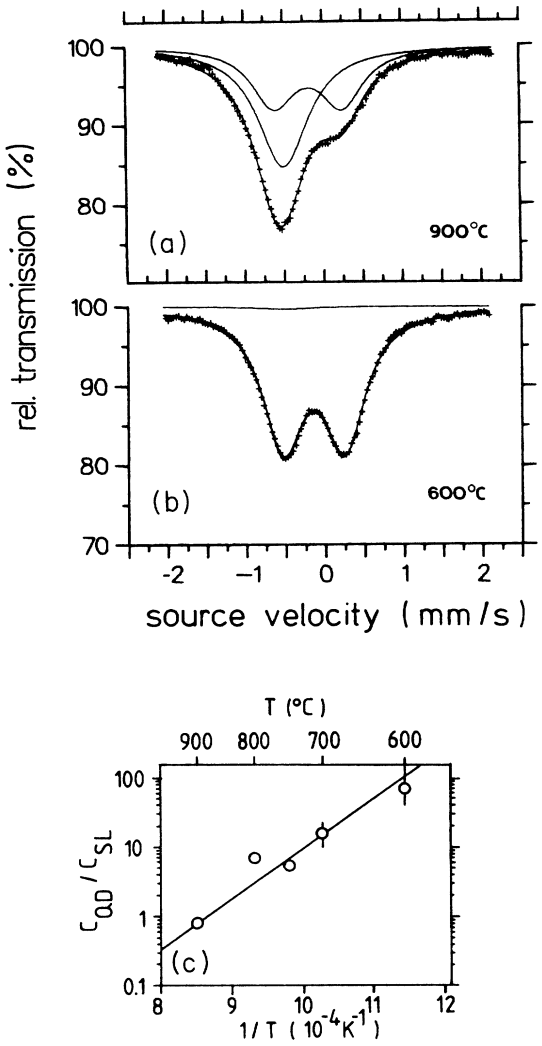

FIG. 7. Simultaneous fit of Mössbauer spectra of ^{57}Co in Si + 10^{20} P-atoms/cm^3 by a single line (SL) with a line position $v=-(0.45\pm0.01)$ mm/s and $\Gamma=0.78$ mm/s, and a quadrupole doublet (QD) with $v=-(0.11\pm0.02)$ mm/s, $\Gamma=0.64$ mm/s, and a splitting $\Delta E_Q=0.79$ mm/s. (a) After annealing at 700 °C, 7 d and 900 °C, 5 min: amplitude $A=7.2\%$ (QD), $A=15.3\%$ (SL). (b) Same as (a) and an additional annealing at 600 °C, 30 min: amplitude $A=16.6\%$ (QD), $A=0.4\%$ (SL). The transformation of the quadrupole doublet into the single line is reversible. The resonance area remains constant indicating equal Debye-Waller factors of the two species. (c) Concentration ratio of the two corresponding Co species vs the temperature calculated from the resonance areas of the Mössbauer spectra. The fit yields $C_{QD}/C_{SL}=(4.2\times10^{-7})\exp[(1.5\pm0.1\text{ eV})/k_BT]$.

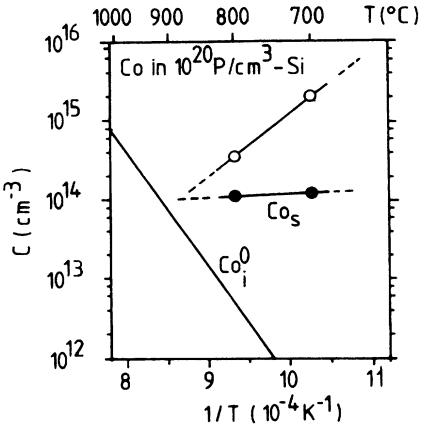

FIG. 8. Temperature dependence of the concentration of the immobile Co species in Si + 10^{20} P-atoms/cm^3 associated with a single line [Co_s(●)] and a quadrupole doublet [Co_sP (○)] in the Mössbauer spectra. For comparison, the concentration of $Co_i^{(0)}$ is shown as well, as given by the solubility in intrinsic Si.

We have applied Mössbauer spectroscopy to study Co in highly-B-doped Si, but—as we will show below—have not found any detectable amount of Co_s, so that $Co_i^{(+)}$ and Co_iB must be the relevant species. We, further, have used known data of the pairing reactions of $Mn_i^{(+)}$ and $Fe_i^{(+)}$ with B to estimate the fraction of pairs at 700 °C to conclude that they can actually dominate the solubility for the highest B content.

Figure 11 presents two Mössbauer spectra of Co in Si + 8×10^{19} B-atoms/cm^3 after in-diffusion of Co at 1200 and 700 °C. The position of the resonance lines in both spectra are characteristic of Co_iB. Small differences compared to the spectra of Bergholz[31] are caused by the

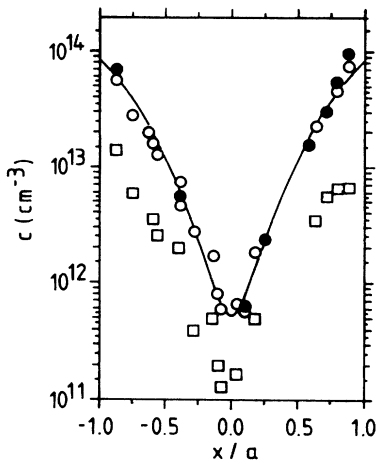

FIG. 9. Concentration profile of the defect associated with DLTS line $L3$ (□, the satellite line in Ref. 3) after diffusion of Mn in Si + 8.5×10^{14} P-atoms/cm^3 at 942 °C for 36 min. The major fraction is interstitially dissolved as measured by the associated DLTS lines $Mn_i^{(0/+)}$ (○) and $Mn_i^{(-/0)}$ (●). The concentration corresponding to $L3$ is proportional to [Mn_i] throughout the diffusion profile.

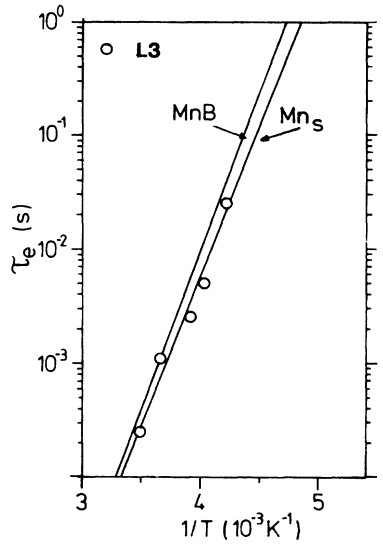

FIG. 10. Comparison of the thermal-emission rate of DLTS line $L3$ (○) with those associated with Mn_iB (Ref. 28) and Mn_s (Ref. 29) (solid lines).

much higher B concentration and are planned to be dealt with in a forthcoming paper.[32] At 1200 °C all Co is dissolved interstitially even for this high B concentration. Our experiment thus demonstrates that also at 700 °C all Co is on interstitial sites either isolated or paired with B. Since complete pairing of Co_i with B occurs during cooling and at room temperautre, the Mössbauer spectra recorded at room temperature, in general, do not reflect the fraction $[Co_iB]/[Co_i]$ at the diffusion temperature.

It is to be expected that the presence of pairs of interstitial impurities and B affects the diffusion coefficient in the same manner as substitutional impurities do in P-doped Si: Local equilibrium between M_i and M_iB has been found to be established even near room temperature as long as M_i is mobile. Since B is a slow-diffusing species compared to the interstitial transition elements $[D(B(700\,°C))\approx 10^{-18}$ cm^2/s (Ref. 33)], M_iB can be regarded as immobile. Its influence on the diffusion can then be described by an effective diffusion coefficient:

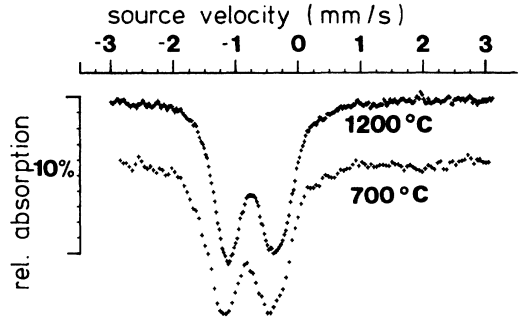

FIG. 11. Mössbauer spectra of ^{57}Co in Si+8×10^{19} B-atoms/cm^3 for annealing temperatures of 700 °C, 15 min and 1200 °C, 30 min, respectively. Both spectra are characteristic of Co_iB pairs and show evidence that Co_s does not contribute to the solubility in B-doped Si.

$$D_{\text{eff}}=\frac{\sum_n [M_i^{(n)}]^{\text{eq}} D_i^{(n)}}{\left[\sum_n [M_i^{(n)}]^{\text{eq}}+[M_iB]^{\text{eq}}\right]} . \tag{4}$$

The formation of pairs between Fe_i and Mn_i with B near room temperature is well established by electron paramagnetic resonance[34] (EPR) and DLTS.[16,18,28] For B concentrations up to some 10^{16} cm^{-3}, the law of mass action is obeyed:

$$[M_iB^{(0)}]/([M_i^{(+)}][B^{(-)}])=K\exp(E_b/k_BT) ,$$

with a binding enthalpy of $E_b=0.65$ eV for Fe_iB (Refs. 15 and 34) and 0.5 eV for Mn_iB (Ref. 29). Extrapolation of this relation to 700 °C and B concentration of 8×10^{19} cm^{-3} yields a ratio $[M_iB^{(0)}]/[M_i^{(+)}]\approx 4$ for Fe and Mn. This indicates that for very high B concentrations the solubility can be affected by this pairing reaction at around 700 °C.

C. Fermi-level dependence of the concentrations of the interstitial and substitutional impurities

1. *Analysis of $C_{\text{tot}}^{\text{eq}}$ and $C_{\text{tot}}^{\text{eq}}D_{\text{eff}}$*

According to the evidence we have presented above for Co, Fe, and Mn, the following species have an influence on the solubility and diffusivity of these elements: $M_i^{(0)}$, $M_iB^{(0)}$, and possibly their positively charged species in B-doped Si, $M_s^{(-)}$, and $M_sP^{(0)}$, and possibly the negatively charged defects $M_s^{(2-)}$ and $M_sP^{(-)}$. For Co a significant contribution of $Co_s^{(+)}$ to the solubility has been excluded by Mössbauer spectroscopy. In this section we present an analysis of $C_{\text{tot}}^{\text{eq}}(E_F)$ and $C_{\text{tot}}^{\text{eq}}D_{\text{eff}}$ in terms of the charge states of the interstitial species. It will be shown that two mobile species, $M_i^{(+)}$ and $M_i^{(0)}$, are required to describe our solubility and diffusion data. Under this assumption the equilibrium concentration of the interstitial species is given by

$$\begin{aligned}[M_i]^{\text{eq}}&=[M_i^{(0)}]^{\text{eq}}+[M_i^{(+)}]^{\text{eq}}\\&=[M_i^{(0)}]^{\text{eq}}\{1+\exp[(G_i^{(0/+)}-E_F)/k_BT]\} .\end{aligned} \tag{5}$$

Since only the interstitial species are expected to contribute to the diffusion, we can write, in addition,

$$\begin{aligned}C_{\text{tot}}^{\text{eq}}D_{\text{eff}}(E_F)&=[M_i^{(0)}]^{\text{eq}}D_i^{(0)}+[M_i^{(+)}]^{\text{eq}}D_i^{(+)}\\&=[M_i^{(0)}]^{\text{eq}}D_i^{(0)}\{1+\exp[(\tilde{G}_i^{(0/+)}\\&\qquad -E_F)/k_BT]\} ,\\ \tilde{G}_i^{(0/+)}&=G_i^{(0/+)}+k_BT\ln(D_i^{(+)}/D_i^{(0)}) .\end{aligned} \tag{6}$$

The analysis of $C_{\text{tot}}^{\text{eq}}D_{\text{eff}}(E_F)$ can give two additional pieces of information.

(1) If species other than the interstitial ones do not contribute to the solubility, i.e., if $[M_i]^{\text{eq}}=C_{\text{tot}}^{\text{eq}}$, the comparison of $\tilde{G}_i^{(0/+)}$ and $G_i^{(0/+)}$ yields $D_i^{(+)}/D_i^{(0)}$.

(2) If $[M_i]^{\text{eq}}\neq C_{\text{tot}}^{\text{eq}}$, charge states of the interstitial impurity are obtained even when the solubility is determined by a different species. Additional spectroscopic

methods are then required to separate the different species involved. By measuring the dependence of the diffusivity and solubility on the Fermi energy, the simultaneous presence of species of the same charge state cannot be separated, e.g., $M_i^{(+)}$ and $M_s^{(+)}$. It is then possible that to some extent a higher diffusion coefficient for $M_i^{(+)}$ is compensated by a contribution of $M_s^{(+)}$ to the solubility:

$$D_{\text{eff}}=[M_i^{(+)}]^{\text{eq}}D_i^{(+)}/([M_i^{(+)}]^{\text{eq}}+[M_s^{(+)}]^{\text{eq}})<D_i^{(+)} . \quad (7)$$

In the following we shall discuss the conclusions for Mn, Fe, and Co that can be drawn from such an analysis of the solubility and diffusion data.

2. *Interstitial Co and Fe in Si*

From the validity of Eq. (2) for Fe and Co [cf. Figs. 5(a) and 6(a)], it follows that at 700 °C their interstitial impurities are mainly neutral for the Fermi level in the upper half of the band gap and have no acceptor levels within the band gap. For B-doped Si our results show that the solubility at 700 °C increases by up to a factor of 40 for Co and a factor of 60 for Fe, whereas the diffusion coefficient decreases by up to a factor of 2 (Fe) or 4 (Co). This shows the existence of $Co_i^{(+)}$ and $Fe_i^{(+)}$, i.e., of a deep donor state at 700 °C. From the slope of $\ln[C_{\text{tot}}^{\text{eq}}(E_F)]$ measured in the lower half of the band gap one derives a single positive charge state of the dominant species [cf. Figs. 5(a) and 6(a)].

In the case of Co that dominant species is $Co_i^{(+)}$ since Co_i and Co_iB have been shown to be the only species in B-doped Si. From a fit of Eq. (6) to our data of $C_{\text{tot}}^{\text{eq}}D_{\text{eff}}$, a value for $\tilde{G}_i^{(0/+)}$ is obtained which agrees within the limits of error with $G_i^{(0/+)}$, as obtained from a fit of Eq. (5) to our data for $C_{\text{tot}}^{\text{eq}}(E_F)$. This implies that $D_i^{(+)}/D_i^{(0)}=1.0\pm0.4$.

For Fe in B-doped Si the slopes $\ln[C_{\text{tot}}^{\text{eq}}(E_F)]$ and $\ln[C_{\text{tot}}^{\text{eq}}D_{\text{eff}}(E_F)]$ coincide and are caused by a single positively charged species. If it is $Fe_i^{(+)}$ only, we obtain $\tilde{G}_i^{(0/+)}\approx G_i^{(0/+)}$ and arrive at the same estimation for the charge-state dependence of the diffusion coefficient as in the case of Co. This estimation is also consistent with experimental findings near room temperature.[36] However, if $Fe_s^{(+)}$ contributes to the solubility appreciably, which we cannot exclude on the basis of our present experimental results, the charge-state dependence of the diffusion coefficient is given by

$$D_i^{(+)}/D_i^{(0)}\approx 1+[Fe_s^{(+)}]^{\text{eq}}/[Fe_i^{(+)}]^{\text{eq}} . \quad (8)$$

3. *Substitutional Fe and Co*

The analysis for the substitutional impurities of Fe and Co is restricted to Fermi levels quite close to the conduction-band edge, where the concentrations of Fe_i and Co_i are only a small part of the solubilities. The dashed line in Fig. 6(a) shows $[Co_s]$ if Co_s is doubly negatively charged. However, due to the lack of data for P concentrations between 5×10^{18} and 10^{20} cm^{-3} a higher charge state of Co_s cannot be excluded. The data of $C_{\text{tot}}^{\text{eq}}(E_F)$ for Fe in P-doped Si would yield an at least triply negative charge state for Fe_s, but a smaller one if Fe_sP contributes appreciably to the solubility.

4. *Interstitial Mn*

For Mn in Si the product $C_{\text{tot}}^{\text{eq}}D_{\text{eff}}$ has been found to be independent of the Fermi level in intrinsic and n-type Si at 854 and 1038 °C. Since, as has been shown previously, $C_{\text{tot}}^{\text{eq}}(T\geq900\,^\circ\text{C})=[Mn_i]^{\text{eq}}$, $Mn_i^{(0)}$ must be the dominant species above 900 °C. The simultaneous increase of $c_{\text{tot}}^{\text{eq}}$ and $C_{\text{tot}}^{\text{eq}}D_{\text{eff}}$ with increasing B concentration shows evidence of a donor level of Mn_i at 854 °C. Taking into account the hypothetical existence of $Mn_s^{(+)}$, the same conclusion for a charge-state dependence of the diffusivity as for Fe can be drawn from the agreement of $\tilde{G}_i^{(0/+)}$ and $G_i^{(0/+)}$ [cf. Eq. (8)]. The drop of D_{eff} with increasing B concentration points to an additional immobile Mn species, possibly Mn_iB (see Sec. III B 2).

5. *Substitutional Mn*

Comparing $C_{\text{tot}}^{\text{eq}}D_{\text{eff}}$ at 700 °C for intrinsic Si and for $Si+5\times10^{18}$ P-atoms/cm^3, one finds that the increase of the solubility with P doping is more than compensated by a decrease of the effective diffusion coefficient. According to the DLTS data, $[Mn_i]^{\text{eq}}\approx0.1C_{\text{tot}}^{\text{eq}}$ in intrinsic Si and, consequently, less than that in the P-doped sample. We suppose that $Mn_s^{(-)}$ dominates the solubility at 700 °C not only for highly-P-doped material, but already for intrinsic Si. The variation of the solubility of this species with the Fermi energy is indicated in Fig. 3(a) by the inclined dashed line.

6. *Electronic instability of interstitial metallic impurities*

Figure 12 presents the temperature dependence of the modified donor levels, $\tilde{G}_i^{(0/+)}$ (open symbols) and $G_i^{(0/+)}$ (solid symbols), for Mn_i, Fe_i, and Co_i. The values of Fe at 900 and 1000 °C ,[25] as well as those for Co at 800 and 900 °C,[27] were derived from a fit to $C_{\text{tot}}^{\text{eq}}(E_F)$ and present upper values for the donor levels. Note that for Co we have found $\tilde{G}_i^{(0/+)}=G_i^{(0/+)}$.

As can be seen from Fig. 12, a sharp drop of $\tilde{G}_i^{(0/+)}(T)$ or $G_i^{(0/+)}(T)$ occurs for all three elements. For Fe_i the value of $\tilde{G}_i^{(0/+)}$ at 700 °C coincides rather well with the value at low temperatures, which can be calculated from DLTS results of the thermal-emission rate and the temperature dependence of the capture coefficient.[20] As a measure of the donor-level shift within the band gap, the ionization entropy $\Delta S_i^{(0/+)}(\ldots,\ldots)=\partial G_i^{(0/+)}/\partial T$ will be used. The ionization state of the donor, which is reached by the transition, and the emitted carrier has to be inserted in $(\ldots,\ldots)$. The ionization entropy for electron-hole generation in the high-temperature region is $\Delta S(e^+,e^-)\approx5.1k_B$, while it is about $2.4k_B$ at room temperature.[21] Van Vechten and Thurmond[37] have argued that for interstitial impurities $\Delta S_i^{(0/+)}(M_i^{(+)},e^-)\approx\Delta S(e^+,e^0)$, or, equivalently, $\Delta S_i^{(0/+)}(M_i^{(0)},e^+)\approx0k_B$. This prediction cannot be confirmed for Fe_i in the low-

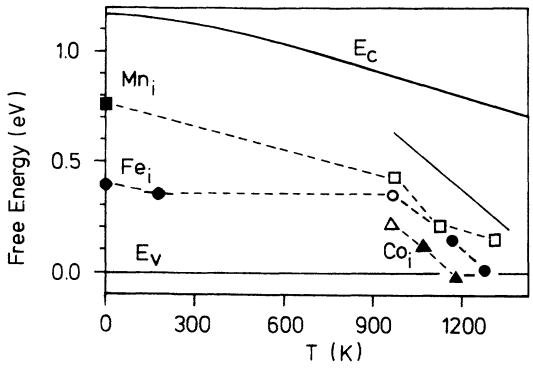

FIG. 12. Temperature dependence of $\tilde{G}_i^{(0/+)}$ (open symbols) and $G_i^{(0/+)}$ (solid symbols) of Mn_i (□), Fe_i (○), and Co_i (△) within the band gap of Si. The values for $\tilde{G}_i^{(0/+)}$ were found to be upper limits for $G_i^{(0/+)}$. The values for $G_i^{(0/+)}$ above 700 °C determined from solubility measurements are upper estimates due to the neglection of $M_s^{(+)}$ or due to the fact that no variation of the solubility with the Fermi energy was found (Ref. 27). For comparison, the single donor level of Fe_i and its temperature dependence at low temperatures (short horizontal line, calculated from Ref. 20) as well as the ionization enthalpy at 0 K are added, as measured by DLTS and Hall effect. The solid line in the high-temperature region shows the dependence of $G_i^{(0/+)}$ on the temperature, as expected for a defect with an ionization entropy of $\Delta S/k_B = 13$.

temperature region, where from DLTS measurements $\Delta S_i^{(0/+)}(Fe_i^{(0)}, e^+)$ values of about $2k_B$ (Ref. 20) can be derived. Due to the small temperature interval, this discrepancy should not be taken too seriously. However, including our results of the donor levels at the diffusion temperature, we can exclude that the donor levels are independent of the temperature with respect to the valence band. For the highest temperatures investigated, it can be concluded that the donor levels for all three impurities are close to the valence band. Note that this conclusion does not depend on the charge-state dependence of the diffusion coefficient.

A clear picture for the temperature dependence of the donor levels between room temperature and diffusion temperatures cannot be established from the present results. Assuming $\tilde{G}_i^{(0/+)} = G_i^{(0/+)}$ for Mn and Fe, the donor level of Fe_i is constant up to 700 °C, whereas for Mn it follows parallel to the conduction band. Obviously, above 700 °C the sharp drop of the donor levels cannot be related to a simple extrapolation of low-temperature results. Above 700 °C the bending of the donor levels to the valence-band-edge results in an ionization entropy $\Delta S_i^{(0/+)}(M_i^{(0)}, e^+)$ for Mn, Fe, and Co larger than $10k_B$. $\Delta S_i^{(0/+)}(M_i^{(+)}, e^-)$ changes sign and becomes negative. In order to develop a model for the temperature dependence of interstitial deep donor levels, measurements of $\Delta S_i^{(0/+)}$ extending to a broader temperature range near room temperature and measurements of the high-temperature donor levels below 700 °C have to be provided.

IV. SUMMARY AND CONCLUSION

We have studied the solubility and diffusion of Mn, Fe, and Co in Si as a function of temperature and doping concentration. The analysis of these data has led us to the following conclusions.

(1) In highly-P-doped Si ([P] $\geq 5\times10^{18}$ atoms/cm^3) and sufficiently low temperatures ($T \leq 900$ °C) the substitutional species of the investigated elements and their pairs with P are dominant. These substitutional species, unlike the interstitial species, introduce one or more acceptor levels into the band gap. The diffusivity of the transition elements in P-doped Si is slowed down by a factor $[M_i^{(0)}]^{eq}/C_{tot}^{eq}$. This means that the substitutional species do not noticeably contribute to transport by diffusion.

(2) The increase of the solubility in highly-B-doped Si at 700 °C relative to intrinsic Si is caused by the singly positively charged interstitial species of Fe, Co, and probably Mn. The diffusion coefficients are comparable with those in undoped Si. Small differences may be due to a pairing reaction of the interstitial 3*d* atoms with B.

(3) The donor levels of Mn_i, Fe_i, and Co_i as a function of temperature shift towards and merge with the valence band above 700 °C. To our knowledge this finding presents the first direct evidence that a point-defect configuration becomes unstable at high temperatures. As a consequence, one has to consider two atomic and electronic configurations associated with the same impurity, one realized at low temperatures ($T < 700$ °C), the other at high temperatures. There is no simple way of extrapolation from one configuration to the other.

(4) The diffusivity of Co_i around 700 °C has been found to be independent of the charge state.

Table IV gives a summary of the different 3*d* impurity-related species found at 700 °C in Si doped with B, intrinsic Si, and Si doped with P. For comparison, the interpretation of the Cu data, as given by Hall and Racette, is shown as well. The differences observed in intrinsic Si are due to the different positions of the deep impurity levels. In B-doped Si the contribution of impurity-boron pairs to the solubility could not be separated accurately from that of $M_i^{(+)}$, but at 700 °C both concentrations seemed to be of about the same value for the highest B doping. In contrast, about 90% of Co_s is found paired with P at 700 °C and the highest P doping. From the overall similarities of the electronic properties, we suppose that for all 3*d* elements listed in Table IV these kinds of pairs present an important contribution to the solubility in *n*-type Si at and below 700 °C, which also explains the different values of the solubility of Cu in P- as compared to As-doped Si.[4]

TABLE IV. 3*d* impurity-related species found in B-doped, P-doped, and intrinsic Si at 700 °C. Identified species are printed in bold. The Cu data represent the interpretation as given by Hall and Racette (Ref. 4). The charge state of M_s is $n \geq 2$, with the exception of Mn in intrinsic Si ($n \geq 1$).

	$T = 700$ °C		
	Si:B	Intr. Si	Si:P
Mn	$\mathbf{Mn_i^{(+)}}$ Mn_iB	$\mathbf{Mn_i^{(0)}}$, $\mathbf{Mn_s^{(-n)}}$	$\mathbf{Mn_s^{(-n)}}$, $Mn_s^{(-n)}P$
Fe	$\mathbf{Fe_i^{(+)}}$, Fe_iB	$\mathbf{Fe_i^{(0)}}$	$\mathbf{Fe_s^{(-n)}}$, $Fe_s^{(-n)}P$
Co	$\mathbf{Co_i^{(+)}}$, Co_iB	$\mathbf{Co_i^{(0)}}$	$\mathbf{Co_s^{(-n)}}$, $\mathbf{Co_s^{(-n)}P}$
Cu	$\mathbf{Cu_i^{(+)}}$	$\mathbf{Cu_i^{(+)}}$	$Cu_s^{(-3)}$

Two final remarks concerning the point-defect instability and the intrinsic point defect that is involved in the reaction between the interstitial and substitutional species of the impurity are in order.

(1) Twenty years ago Seeger and Chick[38] proposed an instability of the self-interstitial in Si in order to account for the large preexponential factor of the Si self-diffusion constant. From high-temperature diffusion data they estimated an entropy of $(13-15)k_B$, which they attributed to a spread of the self-interstitial over several atomic volumes at high temperatures. The authors further proposed that a transition from the high-temperature to a more localized low-temperature configuration occurs at around 900 °C. This is roughly what we observed for Mn_i, Fe_i, and Co_i. Following their considerations, one would expect a change of the solution enthalpies for Mn_i, Fe_i, and Co_i when going below 700 °C, and, possibly, if at all, a minor change of the migration enthalpies. First experiments to determine solubilities below 700 °C failed because of unclear boundary conditions. As far as migration enthalpies are concerned, it has already been mentioned in Sec. III A 2 that for Fe_i the high- and low-temperature values do not differ noticeably.

(2) It has been argued that self-interstitials and vacancies introduce deep levels into the band gap at high temperatures. In intrinsic Si the Au diffusion was found to be controlled by the creation and transport of intrinsic point defect. In P-doped Si, however, from our model of the Co and Fe diffusion it is inferred that their influence is rather small. Hence, in the P-doped material there must be either efficient trapping centers for the Si self-interstitials or a strong enhancement of the vacancy concentration as compared with intrinsic Si. It has been shown recently[27] that an increase of the self-interstitial concentration due to the precipitation of oxygen during annealing of CZ-Si doped with 10^{20} P-atoms/cm^3 at 700 °C leads to a decrease of $[Co_s]$ by about 1 order of magnitude at 700 °C. The diffusion profile can still be described assuming a homogeneous distribution of intrinsic point defects in the specimen. This strongly favors the idea that the vacancy is responsible for the transformation $M_i \rightarrow M_s$ in P-doped Si and means that our measurements are indicative of a vacancy acceptor level at 700 °C. The similarity of the substitutional $3d$ atoms then might have a simple explanation: They form vacancylike states which determine their electronic structure at the diffusion temperature.

Finally, we wish to point out that similar properties for GaAs and Ge are quite likely, since Hall and Racette[4] found a strong increase in the Cu solubility for heavy n-type doping which suggests that this will also be the case for other $3d$-impurity elements in GaAs and Ge.

ACKNOWLEDGMENTS

We would like to thank Dr. J. Utzig of the University of Göttingen for many helpful discussions.

*Present address: Siemens A.G. (HL-TB-32), Otto-Hahn-Ring 6, D-8000 München 83, FRG.

[1]E. R. Weber, Appl. Phys. A **30**, 1 (1983).

[2]K. Graff, in *Semiconductor Silicon 1986,* edited by H. R. Huff, T. Abe, and B. Kolbesen (The Electrochemical Society, Pennington, NJ, 1986), p. 751.

[3]D. Gilles, W. Bergholz, and W. Schröter, J. Appl. Phys. **59**, 3590 (1986).

[4]R. N. Hall and J. H. Racette, J. Appl. Phys. **35**, 379 (1964).

[5]J. D. Struthers, J. Appl. Phys. **27**, 1560 (1956).

[6]M. K. Bakhadyrkanov, S. Zainabidinov, and A. Khamidov, Fiz. Tekh. Poluprovodn. **14**, 412 (1980) [Sov. Phys.—Semicond. **14**, 243 (1980)].

[7]J. Utzig and D. Gilles, in *Defects in Semiconductors 15,* Vols. 38–41 of *Materials Science Forum,* edited by G. Ferenczi (Trans Tech, Aedermannsdorf, Switzerland, 1989), p. 729.

[8]F. Beeler, K. O. Anderson, and M. Scheffler, Phys. Rev. Lett. **14**, 1498 (1985).

[9]A. Zunger, in *Solid State Physics,* edited by H. Ehrenreich and D. Turnbull (Academic, Orlando, FL, 1986), Vol. 39, p. 275.

[10]W. Shockley and J. L. Moll, Phys. Rev. **119**, 1480 (1960).

[11]R. L. Meek and T. E. Seidel, J. Phys. Chem. Solids **36**, 731 (1975).

[12]N. A. Stolwijk, B. Schuster, J. Hölzl, H. Mehrer, and W. Frank, in *Defects in Semiconductors 1982,* edited by C. A. J. Ammerlaan [Physica B&C (Amsterdam) **116B**, 335 (1983)].

[13]F. A. Huntley and A. F. W. Willoughby, Philos. Mag. **28**, 1319 (1973).

[14]W. R. Wilcox and T. J. LaChapelle, J. Appl. Phys. **35**, 240 (1964).

[15]L. C. Kimerling, J. L. Benton, and J. J. Rubin, in *Defects and Radiation Effects in Semiconductors 1980,* IOP Conf. Proc. Ser. No. 59, edited by J. H. Albany (IOP, Bristol, 1981), p. 217.

[16]K. Graff and H. Pieper, in *Semiconductor Silicon 1981,* edited by H. R. Huff, R. J. Kriegler, and Y. Takeishi (The Electrochemical Society, Pennington, NJ, 1981), p. 331.

[17]H. Lemke, Phys. Status Solidi A **64**, 549 (1981).

[18]R. Czaputa, H. Feichtinger, and J. Oswald, Solid State Commun. **47**, 223 (1983).

[19]H. Feichtinger, J. Waltl, and A. Geschwandtner, Solid State Commun. **27**, 867 (1978).

[20]K. Wünstel and P. Wagner, Appl. Phys. A **27**, 207 (1982).

[21]C. D. Thurmond, J. Electrochem. Soc. **122**, 1133 (1975).

[22]J. C. Hensel, H. Hasegawa, and M. Nakayama, Phys. Rev. **138**, 232 (1965).

[23]H. D. Barber, Solid-State Electron. **10**, 1039 (1967).

[24]D. Gilles, Ph.D. thesis, University of Göttingen, 1987.

[25]T. Young, diploma thesis, University of Göttingen, 1982 (unpublished).

[26]D. Gilles and W. Schröter, in *Defects in Semiconductors,* Vols. 10–12 of *Materials Science Forum,* edited by H. J. von Bardeleben (Trans Tech, Aedermannsdorf, Switzerland, 1986), p. 341.

[27]D. Gilles (unpublished).

[28]K. Anderson, diploma thesis, University of Clausthal-Zellerfeld, 1984 (unpublished).

[29]H. Lemke, Phys. Status Solidi A **76**, 223 (1983).

[30]H. Lemke, Phys. Status Solidi A **83**, 637 (1984).
[31]W. Bergholz, in *Defects in Semiconductors 1982,* edited by C. A. J. Ammerlaan [Physica B&C (Amsterdam) **116B**, 312 (1983)].
[32]J. Utzig and D. Gilles (unpublished).
[33]R. B. Fair, in *Impurity Doping Process in Silicon,* edited by F. F. Y. Wang (North-Holland, New York, 1981).
[34]G. W. Ludwig and H. H. Woodbury, in *Solid State Physics,* edited by F. Seitz and D. Turnbull (Academic, New York, 1962), Vol. 13, p. 223.
[35]H. Lemke, Phys. Status Solidi A **64**, 215 (1981).
[36]W. H. Shepherd and J. A. Turner, J. Phys. Chem. Solids **23**, 1697 (1962).
[37]J. A. Van Vechten and C. D. Thurmond, Phys. Rev. B **14**, 3539 (1976).
[38]A. Seeger and K. P. Chick, Phys. Status Solidi **29**, 455 (1968).